Three term Amplitude-Versus-Offset (AVO) inversion revisited by curvelet and wavelet transforms

Gilles Hennenfent and Felix Herrmann, EOS, University of British Columbia

Summary

We present a new method to stabilize the three term AVO inversion using curvelet and wavelet transforms. Curvelets are basis functions that effectively represent otherwise smooth objects having discontinuities along smooth curves. The applied formalism explores them to make the most of the continuity along reflectors in seismic images. Combined with wavelets, curvelets are used to denoise the data by penalizing high frequencies and small contributions. This approach is based on the idea that rapid amplitude changes along the ray-parameter axis are most likely due to noise. The AVO inverse problem is linearized, formulated and solved for all (x, z) at once. Using densities and velocities of the Marmousi model to define the fluctuations in the elastic properties, the performance of the proposed method is studied and compared with a conventional method. We show that our method better approximates the true data after the denoising step, especially when noise level increases.

Introduction

In oil exploration industry, reflection seismology is widely used to image the subsurface structure. Pressure waves are emitted by a source at the surface into the Earth. Due to the property contrast between two consecutive layers, one part of the energy is transmitted and the other is reflected back up to be detected by receivers at the surface. Signals are recorded over a range of source and receiver offsets.
The reflectivity varies significantly along the ray-parameter axis and it can be used to make inferences about the properties of the layers. This technique is called Amplitude Versus Offset (AVO) inversion. Due to the ill-conditioned nature of the inverse problem, it is difficult to obtain accurate estimates for these properties. In other words, a small amount of noise may lead to large errors in the estimates.

In the first part of this paper, we present how curvelets and wavelets can be used to stabilize the three term AVO inversion. We explore the fact that seismic images can be efficiently represented by curvelets since discontinuities (i.e. interfaces between layers) occur along curves. By working on the coefficients of the curvelet transform instead of the data, we consider the point as part of an environment in opposition to an isolated point. Consequently, information regarding the near-neighborhood of each point can be used to better denoised the data. Intuitively, the curvelet transform can be seen as a local extraction of major events combined with a local averaging of the noise. Based on the idea that rapid amplitude changes along the ray-parameter axis result from noise (Kuehl and Sacchi, 2003), we denoise the data by thresholding high frequencies and small contributions. The denoised data are inverted for all (x, z) at once.

In a second part, we illustrate our method using densities and velocities of the Marmousi model to define the fluctuations in the elastic properties. The denoised data and the recover model are compared with results obtained by using a conventional method where only wavelets could have been used to smooth AVO responses and the inverse problem were carried out point-by-point.

Wavelet and curvelet transforms

Multi-resolution transforms have proven to be successful in signal processing applications (Mallat, 1999). Among these, wavelets are probably the most famous and widely used. Because they are localized and multi-scale, their ability to preserve and characterize point singularities in a noisy signal is proven to be better than discrete Fourier transform. However their poor orientation selectivity prevents to represent higher-dimensional singularities effectively.

The curvelet transform is a relatively new multi-scale transform with strong directional character in which elements are strongly anisotropic at fine scales, with effective support shaped according to the parabolic scaling principle length^2 $\sim$ width (Candes and Donoho, 1999). Curvelets provide stable, efficient, and near-optimal representation for seismic data with reflectors on piece-wise smooth curves.

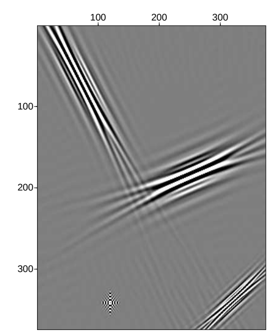

Figure 1: Some curvelets at different scales (Courtesy Emmanuel Candès)

AVO inversion of PP data

At position (x_i, z_i), the linearized Zoeppritz equation for PP reflection coefficients (RCs) can be written for small angles and contrasts as (Aki and Richards, 1980)

$$R_{pp}(p) = \frac{1}{2}(1 - 4\bar{c}_S^2 p^2 \frac{\Delta\rho}{\bar{\rho}}) + \frac{1}{2\cos^2\theta}\frac{\Delta c_P}{\bar{c}_P} - 4\bar{c}_S^2 p^2 \frac{\Delta c_S}{\bar{c}_S} \quad (1)$$

where ρ is the density, c_P (resp. c_S) the velocity of P-waves (resp. S-waves), and the ray parameter $p \times \bar{c}_P = \sin\theta$.

Using the following substitutions (van Wijngaarden, 1998) for the acoustic impedance Z

$$\frac{\Delta Z}{\bar{Z}} = \frac{\Delta c_P}{\bar{c}_P} + \frac{\Delta\rho}{\bar{\rho}}, \tag{2}$$

and for the shear modulus μ

$$\frac{\Delta\mu}{\bar{\mu}} = \frac{\Delta\rho}{\bar{\rho}} + 2\frac{\Delta c_S}{\bar{c}_S}, \tag{3}$$

the RCs can be approximated by

$$R_{pp}(p) \approx \frac{1}{2}\frac{\Delta Z}{\bar{Z}} + \left[\frac{1}{2}\frac{\Delta c_P}{\bar{c}_P} - 2\left(\frac{\bar{c}_S}{\bar{c}_P}\right)^2\frac{\Delta\mu}{\bar{\mu}}\right]\bar{c}_P^2 p^2. \tag{4}$$

For N ray parameters, the local forward model for the seismic data becomes

$$d_{pts} = \begin{pmatrix} 1/2 & \frac{1}{2}\left(\frac{\bar{c}_P^2 p_1^2}{1-\bar{c}_P^2 p_1^2}\right) & -2\frac{\bar{c}_S^2}{\bar{c}_P^2}\bar{c}_P^2 p_1^2 \\ \vdots & \vdots & \vdots \\ 1/2 & \frac{1}{2}\left(\frac{\bar{c}_P^2 p_N^2}{1-\bar{c}_P^2 p_N^2}\right) & -2\frac{\bar{c}_S^2}{\bar{c}_P^2}\bar{c}_P^2 p_N^2 \end{pmatrix} m_{pts} + n_{pts} \tag{5}$$

with

$$d_{pts} = \Big(R_{pp}(p_1), \ldots, R_{pp}(p_N)\Big)^T, \tag{6}$$

$$m_{pts} = \left(\frac{\Delta Z}{\bar{Z}}, \frac{\Delta c_P}{\bar{c}_P}, \frac{\Delta\mu}{\bar{\mu}}\right)^T \tag{7}$$

d_{pts} is the seismic data (i.e. reflectivities) for one point in the space domain along the ray parameter axis, m_{pts} the model (i.e. elastic properties) for this point, and n_{pts} the noise. Without loss of generality, we will assume the additive noise to be white Gaussian with the same mean and variance for all the points.

In the conventional approach for the estimation of contrasts in elastic properties, one carry out for each point of the space domain

$$\min_{m_{pts}} ||d_{pts} - K_{pts} m_{pts}||^2 \tag{8}$$

where K_{pts} stands for the linearized reflection operator. By repeating the process, the sections for each contrast parameter are built point-by-point. Due to the ill-conditioned nature of the inverse problem, it is difficult to obtain accurate estimates for the contrast parameters.

We, on the other hand, consider the RC cube as a whole even though it is still ill-conditioned. The seismic data becomes

$$d = Km + n \tag{9}$$

where d is the whole RC cube, K the corresponding linearized reflection operator, m the 3 contrast parameter sections, and n the white Gaussian noise. In this case, one can introduce in the cost function to be minimized global *a priori* knowledge in order to help to converge to the model. Sacchi propose to minimize the following cost function (Kuehl and Sacchi, 2003)

$$F(m) = ||W(d - Km)||^2 + \lambda^2||\partial_p(Km)||^2 \tag{10}$$

where W is a (diagonal) weighting operator and λ^2 a tradeoff parameter depending on the noise level. The second term in the objective function imposes a relative smoothing constraint in the ray parameter domain but it doesn't include any *a priori* information on the lateral continuity along reflectors.

Our concern is to account for both smoothness in the ray-parameter domain and along edges in the space domain. The general idea is to use curvelets in the space domain (2-D) to benefit from information regarding edges and wavelets in the ray-parameter domain (1-D) to denoise AVO responses.

Improvement of the data SNR

The denoising of the data does not require the problem to be linearized. Instead of using a smoothing constraint term in the cost function, we use the multi-scale property of wavelets. The smoothness condition is then equivalent to penalize high frequency and small contribution coefficients of the wavelet transform in the ray-parameter domain by thresholding. These coefficients are most likely due to noise in the data. But first, to make the most of the continuity along reflectors, we take a curvelet transform in the space domain. This operation can be seen as a local averaging of the noise and a very efficient way to sparsely represent our signal. Chronologically speaking

$$C_{xz}d = C_{xz}Km + C_{xz}n \tag{11}$$

$$W_p C_{xz}d = W_p C_{xz}Km + W_p C_{xz}n \tag{12}$$

$$\hat{\tilde{d}} = \Theta_\Gamma(W_p C_{xz}d) \approx W_p C_{xz}Km \tag{13}$$

where C_{xz} is the curvelet transform in the space domain, W_p the wavelet transform in the ray-parameter domain, $\Theta_\Gamma(.)$ a hard thresholding with a threshold level Γ, and $\hat{\tilde{d}}$ the approximate of the data in the curvelet-wavelet domain.

Γ is estimated by evaluating the composition of curvelet and wavelet transforms of a few standard white noise signals (Starck et al., 2002)

$$\Gamma \propto \left[\frac{1}{Q}\sum_{i=1}^{Q}\Big(W_p C_{xz}N(0,1)\Big)^2\right]^{\frac{1}{2}} \tag{14}$$

Since the amplitudes are important in our case, it is important to only consider hard thresholding, which preserve the amplitudes unlike soft thresholding. Note also that the threshold level Γ does not prevent strong events in the high frequencies to remain. Thus, it is possible to apply this method to data containing post-critical angles.

From Eq. 13, by taking the inverse wavelet and inverse curvelet transforms, one have an approximation of the data $\hat{d}$

$$\hat{d} = C_{xz}^{-1}W_p^{-1}\Theta_\Gamma(W_p C_{xz}d) \approx Km. \tag{15}$$

At this point, we assume that the noise was removed from the data and we carry out the inverse problem using $\hat{d}$ to obtain the recovered model m_r

$$m_r = \min_m ||\hat{d} - Km||^2 \tag{16}$$

Example

To illustrate our method, densities and velocities of the Marmousi model are used to define the fluctuations in the elastic properties. Two noisy data sets d_1 and d_2 are built. d_1 (resp. d_2) has a $SNR = 0\ dB$ (resp. $SNR = 6\ dB$). Without loss of generality, we will assume the additive noise to be white Gaussian. As a first approximation, small angle and small contrast assumptions are made. In other words, the dip is not corrected.

Both data sets are processed using our method and a conventional one. The conventional method considers each point separately as formulated in Eq. 5 and imposes a smoothing condition on their AVO response. In this case, we apply directly on the data a wavelet transform in the ray-parameter domain (Eq. 17) and hard threshold (Eq. 18) with a threshold level $\mu = \sigma\sqrt{2\log_e N}$ where σ is the standard deviation of the noise and N the number of data samples (**?**). We finally get the approximated data using the conventional method by taking the inverse wavelet transform in the ray-parameter domain (Eq. 19).

$$W_p d_{pts} = W_p K_{pts} m_{pts} + W_p n_{pts} \tag{17}$$

$$\hat{d}'_{pts} = \Theta_\mu(W_p d_{pts}) \approx W_p K_{pts} m_{pts} \tag{18}$$

$$\hat{d}_{pts} = W_p^{-1}\Theta_\mu(W_p d_{pts}) \approx K_{pts} m_{pts} \tag{19}$$

In Fig. 2, we can see that our method to denoise the data outperforms the conventional method in the sense that our approximated data is closer to the true data. This is especially true for the d_1 where the noise level is higher.

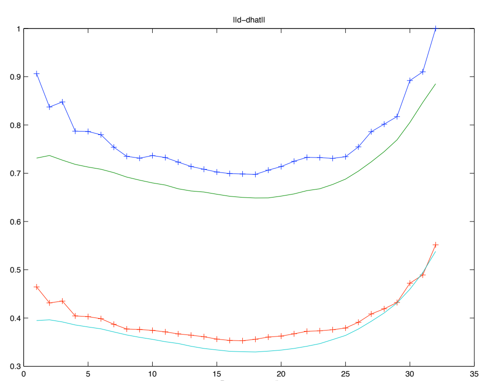

Figure 2: Normalized misfit $||d - \hat{d}||$ function of the ray-parameter #. +- lines represent misfits using the conventional methods, straight lines misfits using our method. In the upper part, the misfits are related to d_1, in the bottom part to d_2.

For a better understanding, four sample reflectors were chosen to compare the methods (Figs 3 & 4). For high level of noise, the conventional method is not able to make the difference between the signal and the noise whereas our method does due to the neighborhood-effect introduced by curvelets. An illustrative example is reflector 3 in Fig. 3 around ray parameter #20. The conventional method tends to follow the noise whereas our method stays close to the true data.

Discussion

We developed and demonstrated in this paper a new method that uses curvelet and wavelet transforms to stabilize the three-term AVO inversion. Our method was successfully compared with a conventional method on synthetic data for the denoising and the neighborhood-effect of curvelets was highlighted.

By using the curvelet transform, we can determine and correct for the dip.

Our method can be applied to data with post-criticals angles without any problem.

Acknowledgement

The authors would like to thank Emmanuel Candès and David Donoho for making their Digital Curvelet Transform via Unequally-spaced Fourier Transforms available for evaluation. This work was in part financially supported by a NSERC Discovery Grant.

References

Aki, K., and Richards, P. G., 1980, Quantitative seismology: Theory and methods: W. H. Freeman and Co.

Candes, E., and Donoho, D., Curvelets: A surprisingly effective nonadaptive representation of objects with edges:, Technical report, Caltech, 1999.

Candes, E., and Donoho, D., 2000, Recovering Edges in Ill-Posed Inverse Problems: Optimality of Curvelet Frames.

Kuehl, H., and Sacchi, M. D., January-February 2003, Least-squares wave-equation migration for avp/ava inversion: Geophysics, **68**, no. 1, 262–273.

Mallat, S., 1999, A wavelet tour of signal processing: Academic Press.

Starck, J., Candes, E. J., and Donoho, D. L., June 2002, The curvelet transform for image denoising: IEEE Trans. Image Proc., 670–684.

van Wijngaarden, A.-J., 1998, Imaging and characterization of angle-dependent seismic reflection data: Ph.D. thesis, Delf University of Technology.

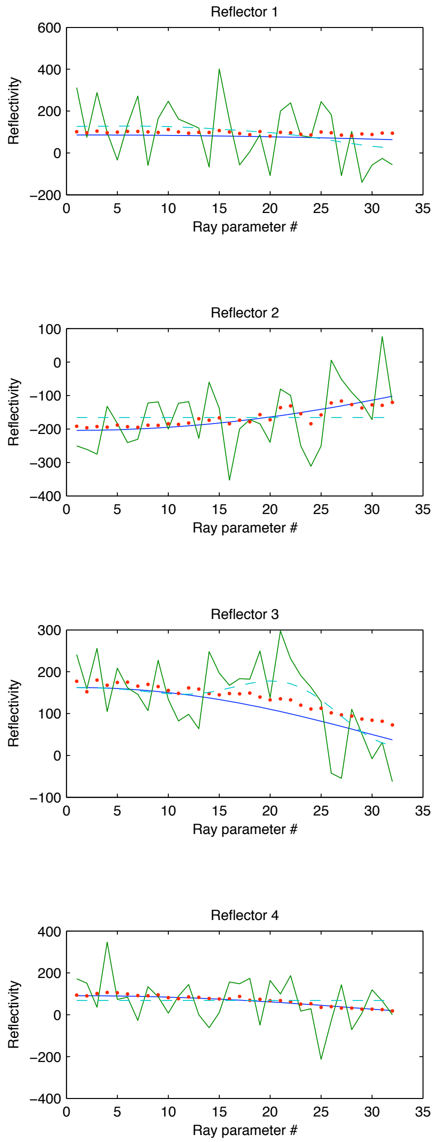

Figure 3: Denoised data using either our method (dotted line) and a conventional one (dashed line) compared against each other with respect to the true data and the noisy data d_1 ($SNR = 0$) on the four sample reflectors.

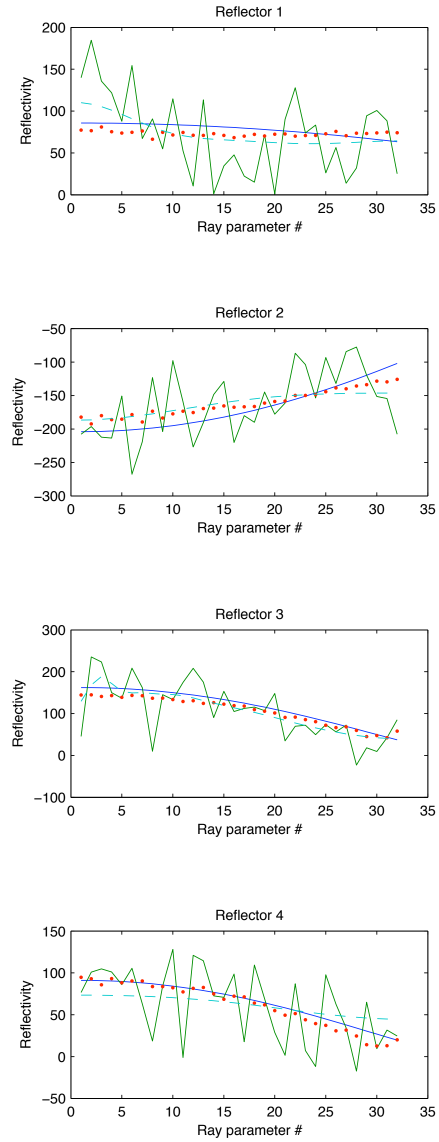

Figure 4: Denoised data using either our method (dotted line) and a conventional one (dashed line) compared against each other with respect to the true data and the noisy data d_2 ($SNR = 6$) on the four sample reflectors.